EPJ Photovoltaics **14**, 29 (2023)
© A. Fischer et al., Published by EDP Sciences, 2023
https://doi.org/10.1051/epjpv/2023023

Available online at:
www.epj-pv.org

Special Issue on 'EU PVSEC 2023: State of the Art and Developments in Photovoltaics', edited by Robert Kenny and João Serra

REGULAR ARTICLE

OPEN ACCESS

Impact of organic particles from wafer handling equipment on silicon heterojunction pseudo-efficiency

Andreas Fischer*, Ioan Voicu Vulcanean, Sebastian Pingel, and Anamaria Steinmetz

Fraunhofer Institute for Solar Energy Systems (F-ISE), Freiburg, Germany

Received: 6 June 2023 / Received in final form: 8 August 2023 / Accepted: 13 September 2023

Abstract. Within this paper a systematic analysis of particle transfer onto SHJ Solar cell precursors by handling with suction cups and the impact on the pseudo efficiency is presented. The study establishes a correlation between particle area coverage and a resulting loss of pseudo solar cell parameters. The analysis was carried out on one hand by means of SEM measurements at the contact points between suction cup and wafer to quantify particle transfer and on the other hand by means of suns photoluminescence imaging measurements to evaluate the resulting losses. It is shown that the choice of contact material and the wafer temperature have a significant influence on the transferred particle number, their size and the resulting particle area coverage. A local electrical defect was observed at these particle-rich spots, which also affected a larger area around this insufficiently passivated region. This had a significant negative effect on the pseudo efficiency, which is more pronounced for increasing particle area coverage. If the particle density is increased by 0.1% within an area of 800 mm^2, the pseudo efficiency in this area decreases by almost 1.2$\%_{Relative}$. The correlation found can be used to predict an efficiency loss using standard photoluminescence images.

Keywords: SHJ / handling / passivation defects / particles

1 Introduction

In the photovoltaic industry, it was recognized early that a high degree of automation is essential to ensure quality in mass production and to minimize costs [1,2]. The handling of components with sensitive or functional surfaces is a major challenge [3], with automated handling and the associated gripping technology being particularly affected [4]. Surface sensitive cell concepts based on passivated selective contacts are expected to gain significant market share over the next decade. At the same time, the throughput of conventional industrial production equipment will continue to increase to over 7000 wafers per hour [5]. For these cell concepts, such as silicon heterojunction, the requirements for the purity and nature of the silicon surface, which later becomes the interface between the silicon base substrate and the passivation layer, are increasing. As a starting point, a clean, defect-free, and specifically H-terminated silicon surface is required prior to passivation [6]. To meet these interface requirements, a new challenge is added concerning handling of wafers: The handling system, which typically consists of vacuum or Bernoulli grippers and conveyor belts, must not interfere with the sensitive, cleaned, and potentially hot wafer surface. It is therefore necessary to thoroughly analyze handled wafers between process steps to identify handling defects, localize their cause, and estimate the resulting efficiency loss. In [7,8] it is described that amorphous silicon (a-Si) passivation defects resulting from grippers are mainly caused by particle transfer. This particle transfer led to a characteristic imprint on assigned lifetime calibrated photoluminescence (PL) images. A reduction of transferred particles reduced or even avoided these imprints. Based on the reduced signal intensity of the lifetime calibrated PL images due to particle contamination, it was concluded that lateral recombination currents occur, and the overall passivation level will be lowered, resulting in a reduced cell efficiency. A similar observation was seen in [9], where cleaning of conveyor belts and grippers for the handling of wafers before passivation resulted in an efficiency gain of about 0.15% absolute. In [10] J–V measurements on manufactured silicon heterojunction solar cells and SunsPL imaging measurements on solar cell precursors showed, that local insufficient passivated regions caused by handling before passivation not only cause a local electrical defect at the point of handling, but also affect a large area around the locally insufficient passivated region. This had a significant negative effect on all solar cell parameters and pseudo cell parameters. It was concluded, that the (pseudo) fill

* e-mail: andreas.fischer@ise.fraunhofer.de

This is an Open Access article distributed under the terms of the Creative Commons Attribution License (https://creativecommons.org/licenses/by/4.0), which permits unrestricted use, distribution, and reproduction in any medium, provided the original work is properly cited.

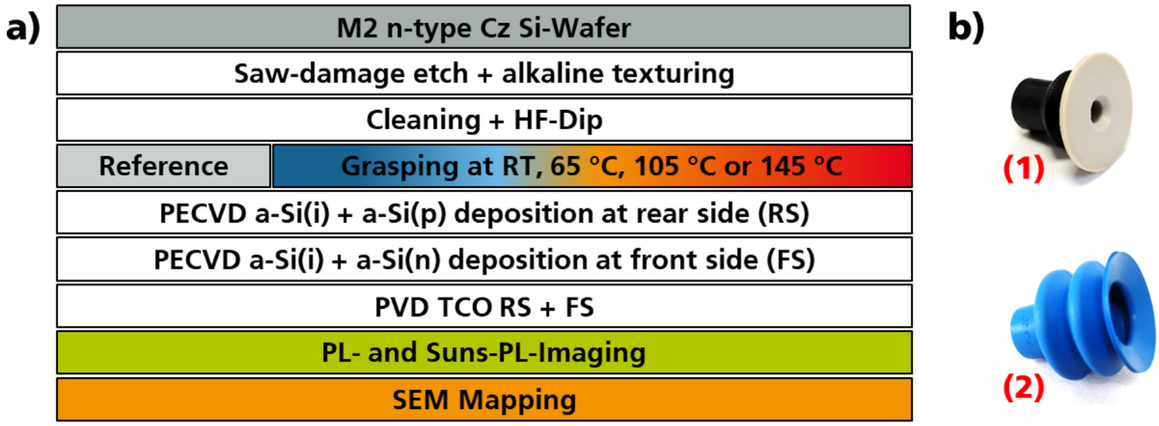

Fig. 1. a) Process flow of the experiment for the study of particles and their influence on SHJ solar cell pseudo-efficiencies, b) Suction cups used, with either PEEK (1) or PU (2) as contact material.

factor was the main parameter for a reduced (pseudo) efficiency. In this context a correlation between particle area coverage and a resulting loss of the pseudo efficiency is investigated. This is done by using the two most widely used materials for handling in the PV industry. These are Polyurethane (PU), a common conveyor belt material, and Polyetheretherketone (PEEK), a common contact material for vacuum and Bernoulli grippers. The results are used to introduce a procedure for estimating and classifying local intensity losses in PL images due to organic particles left by wafer handling equipment with respect to their effect on pseudo-efficiencies.

2 Experimental details

The process flow and the vacuum grippers used in this study are shown in Figure 1. Textured and cleaned 180 µm thick (as-cut), 1 Ω cm, *n*-type silicon Cz wafers were handled by four vacuum grippers, excluding the reference group. Handling was performed between wet chemical cleaning and plasma enhanced chemical vapor deposition (PECVD) of a-Si layer stacks. The wafers were handled with suction cups at various temperatures up to 145 °C. The contact material of the suction cups was either the elastomer Polyurethane (PU) or the semi-crystalline thermoplastic Polyetheretherketone (PEEK). After PECVD deposition, a transparent conductive oxide (TCO) was applied to the rear and front of the wafer by physical vapor deposition (PVD). These finished SHJ solar cell precursors were measured by PL imaging and SunsPL imaging [11]. Characteristic defects seen in the PL images were further analyzed by SEM. To create an image around the handling defect, 840 SEM images per sample were measured and stitched together at a magnification of 2000. Particles seen in this image were counted and measured for an area of 50 µm × 50 µm. To obtain a particle area coverage value (n) following equation (1) was applied.

$$n = \frac{\text{particle count} * \text{particle size}}{50\mu m * 50\mu m}. \tag{1}$$

Energy dispersive X-ray spectroscopy (EDX) was used to assign the particles found to the contact material. For the SunsPL measurement, implied voltage (iV_{suns}) calibrated PL images were generated at illumination intensities between 0.005 and 1 suns. The implied open circuit voltage (iV_{OC}) refers to iV_{suns} measured at one sun. For each illumination intensity, a corresponding pseudo current density (I_{suns}) was calculated by $I_{suns} = I_{SC} * (1 - \text{suns})$, while the short-circuit current density (I_{SC}) value was obtained from J-V measurements of further processed and metallized SHJ solar cell precursors. Each of these calculated I_{suns} values was multiplied by the data points (pixels) of the iV_{suns} image obtained at the corresponding illumination intensity, resulting in a pseudo power image. The pseudo power image consisting of pixels with the highest global average power value was further used as the image at maximum power point ($P_{MPP,SunsPL}$). To obtain a pseudo fill factor (pFF) image the following equation (2) was applied pixel by pixel.

$$pFF(x,y) = \frac{P_{MPP,SunsPL}(x,y)}{iV_{OC}(x,y) * I_{SC}} = \frac{iV_{MPP}(x,y) * I_{MPP,SunsPL}}{iV_{OC}(x,y) * I_{SC}}. \tag{2}$$

In the next step, the pixels of pseudo efficiency images (η_{Pseudo}) were calculated using the following equation (3).

$$\eta_{pseudo}(x,y) = \frac{pFF(x,y) * I_{SC} * iV_{OC}(x,y)}{P_{in}}. \tag{3}$$

It should be noted that the assumption of a global average value for I_{SC} and $I_{suns,\ MPP}$ used for all pixels does not correspond to reality. Due to the longer diffusion length of the minority carriers under MPP conditions than under open-circuit voltage conditions, the quotient of iV_{MPP} values to iV_{OC} values is higher in the maximum defect than in the surrounding areas. Therefore, using global average $I_{MPP,\ SunsPLI}$ and I_{SC} values for the pFF calculation for all pixels will result in an overestimation of the pFF values and therefore of the η_{Pseudo} at these points. Furthermore, for

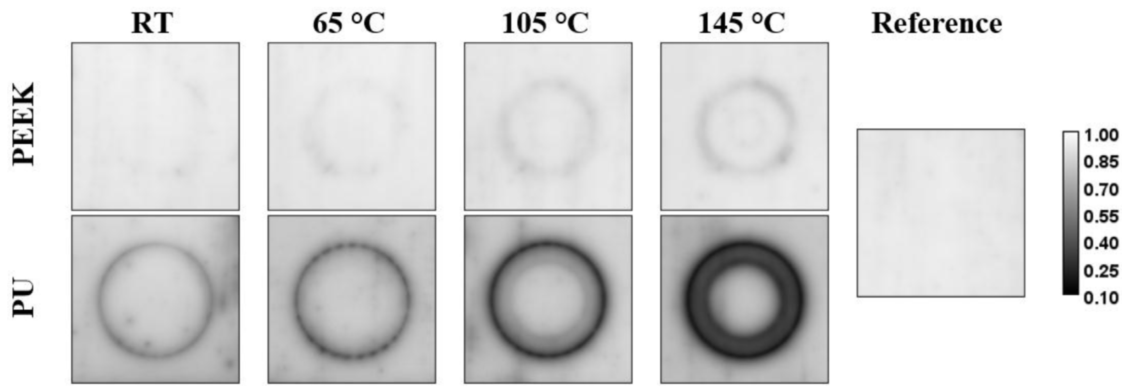

Fig. 2. Region of interest of normalized and averaged PL images in the grasped area.

comparison with real values, the I_{SC} value would have to be corrected upwards by a shading factor. This is because the SunsPL measurements are made on solar cell precursors without metallization. As all values used in this work are later normalized, this does not affect the results. Another implication of this is the lack of a final curing step. However, since the defects under investigation are caused by particle carryover prior to passivation, and the silicon surface cannot be passivated at these locations, no further improvement is expected from a curing step.

3 Results and discussion

3.1 Correlation of PL intensity and particle density

In this section, the number and size of particles carried over from the suction cups, and thus the particle area coverage in the handled area, are measured, calculated, and correlated with normalized PL intensities. Figure 2 shows the region of interest of characteristic defects from normalized averaged PL images. These images were generated from at least eight PL images, with each PL image normalized to its maximum value. PEEK as a contact material induced a circular defect in the PL image, which is visible at handling temperatures of 65 °C and higher. With increasing temperature, lower PL intensities are obtained in the circular defect. Handling at room temperature showed no circular defect in the corresponding averaged PL image. For wafers handled with PU as contact material, a circular defect is already visible at RT. Again, lower PL intensities are measured with increasing temperature. Compared to wafers handled with PEEK as contact material, lower PL intensities are seen for wafers handled with PU. Given this information, higher particle transfer can be expected with increasing temperature, with particle transfer generally predicted to be higher for PU than for PEEK as the contact material.

Figure 3 shows an exemplary SEM image at the location of minimum PL intensities for samples handled with PEEK as contact material at 105 °C. This image has an area of $50\,\mu m \times 50\,\mu m$ and is a representative section with particles from a stitched SEM image containing 840 individual SEM images. The particles highlighted in yellow are located at the tips of the pyramids and have an average size of $0.6\,\mu m^2$. These particles are in a stripe with an

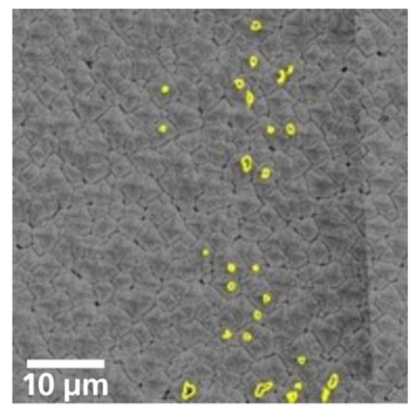

Fig. 3. Exemplary SEM image with a cross section of $50\,\mu m \times 50\,\mu m$ of the grasped area of a wafer handled by suction cups with PEEK as the contact material at a temperature of 105 °C.

average width of $22\,\mu m$ and form a ring that can be seen as low intensity area in the PL image. The material of these particles can be associated with the contact material and is independent of the handling temperature. The elements of PEEK ($C_{19}H_{12}O_3$), carbon (C) and oxygen (O), are always present in the corresponding EDX spectrographs (Fig. 4). The peak for silicon (Si) originates from the wafer surface.

Figure 5 shows a section of a stitched image and a $50\,\mu m \times 50\,\mu m$ surface area at the location of minimum PL intensities for samples handled with PU as the contact material at 105 °C. A dark stripe with an average width of $266\,\mu m$ can be seen in the stitched image. This stripe is a section of the ring that can be seen as low intensity area in the PL image. The reason for this dark stripe is the presence of transferred particles, which are highlighted in the image taken from the inside of the dark stripe. No particles were found outside the dark stripe. Again, these particles are mainly located at the tips of the pyramids. For this handling temperature, an average particle count of 326 with an average particle size of $0.09\,\mu m^2$ was measured. As with PEEK, the material of these particles can be associated with the contact material and is independent of the handling temperature. Corresponding EDX spectrographs (Fig. 6) always show the elements for PU (Urethan group (–NH–CO–O–), namely carbon (C), nitrogen (N), and oxygen (O).

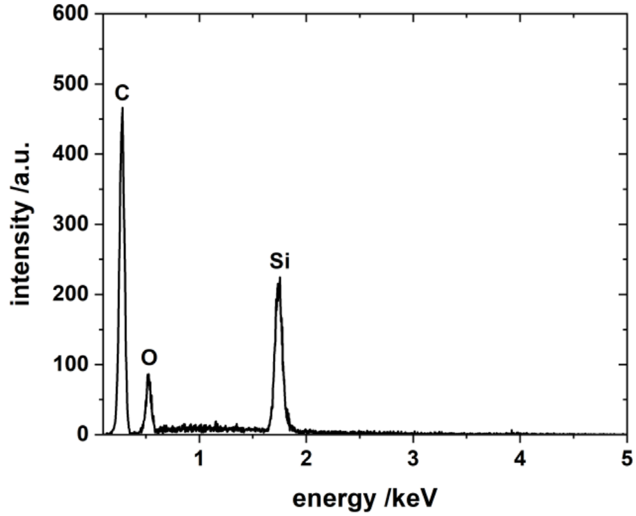

Fig. 4. EDX spectrum of a particle found in the grasped area of a wafer handled by suction cups with PEEK as the contact material at a temperature of 105 °C.

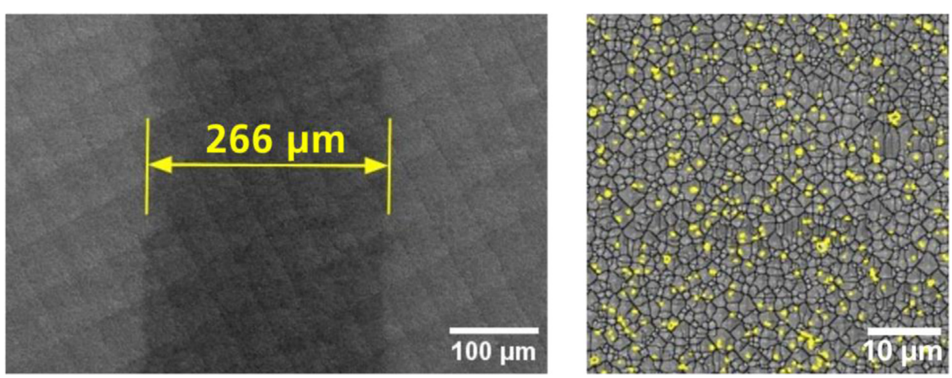

Fig. 5. Part of a stitched SEM image of the grasped area of a wafer handled by suction cups with PU as the contact material at a temperature of 105 °C (left). Exemplary SEM image within the dark stripe with a cross-section of $50\,\mu m \times 50\,\mu m$ (right).

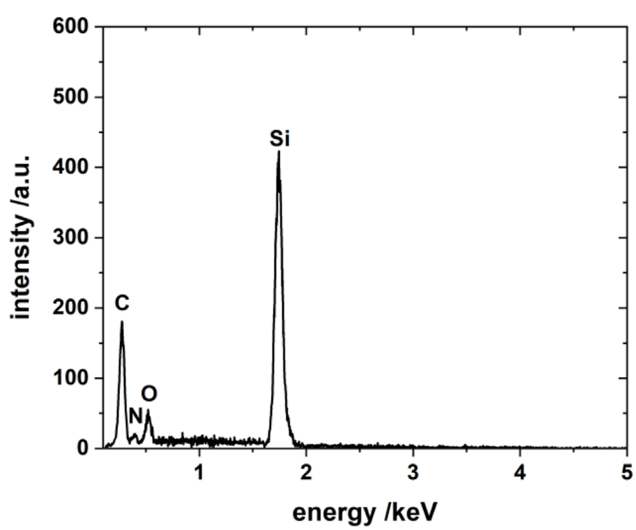

Fig. 6. EDX spectrum of a particle found in the grasped area of a wafer handled by suction cups with PU as the contact material at a temperature of 105 °C.

Table 1. Values for particle number, particle size, width of particle stripe and particle density of the SEM analysis for both contact materials and all handling temperatures.

		Average number of particles in an area of 50 μm × 50 μm	Average particle size (μm^2)	Width of particle stripe (μm)	Particle area coverage for the circular defect (%)
PEEK	65 °C	6	0.71	20	0.01
	105 °C	21	0.59	22	0.03
	145 °C	41	0.31	33	0.05
PU	RT	29	0.23	200	0.20
	65 °C	91	0.15	250	0.52
	105 °C	326	0.09	266	1.13
	145 °C	442	0.1	266	1.71

The results of this SEM analysis for both contact materials and all handling temperatures are shown in Table 1. Since no circular defects have been observed on wafers that have been handled at RT with PEEK as the contact material, no values can be given for this. As the handling temperature increases, the average number of particles and the width of the stripe containing particles increase. The opposite is true for the average particle size, which decreases with increasing temperature. The mechanism of particle transfer during static polymer-silicon contact is still unexplored, and the experiments available in the literature unfortunately cannot provide any information on the mechanism [12]. Studies exist mainly on friction pairings where friction leads to wear. In PEEK systems, the roughness of the contacting surface seems to partially determine the wear mechanisms. Ovaert et al. [13] found that above an optimum roughness value, fatigue and abrasive wear become increasingly dominant, which is the case for textured silicon surfaces in PV. Abrasive wear of polymers depends mainly on their hardness, as described in the Archard model [14]. The model assumes that wear occurs at the interface and that the volume of wear caused by a single roughness peak depends on the depth of plastic deformation of the polymer. The hardness of PEEK is temperature dependent, so that it gets softer when the temperature increases [15]. It can be assumed that there was no plastic deformation of the PEEK inserts used at RT, resulting in no transferred particles on the silicon surface. Increasing the temperature caused plastic deformation at the tips of the pyramids due to reduced material hardness, resulting in particle transfer. When the temperature was further increased, in consequence reducing the hardness, a greater number of particles were transferred. The wear of elastomers such as PU is still poorly understood [16]. For a rough estimate, the Holm-Archard equation can be used to describe adhesive wear. For adhesive wear, the volume worn is inversely proportional to the hardness, as for abrasive wear. For elastomers, the hardness is replaced by the average stress in the microcontacts. If this is less than the hardness of the contacting surface, which is the case in this work, elastic deformation can be assumed. To characterize rubber wear, the so-called abradability is often used as the ratio of the worn volume to the loss energy. It is inversely proportional to the imaginary part of the complex modulus, which is temperature dependent [16]. Therefore, it can be assumed that as the temperature increases, more particles reach the surface, as shown experimentally. Translating these results to the industrial production of SHJ solar cells, it can be said that handling at room temperature with suction cups with PEEK as contact material does not lead to increased particle transfer. At elevated wafer temperatures, particle transfer could be further reduced by using more heat resistant contact materials, such as ceramics. For conveyor belts, the choice of materials is limited. Soft materials such as PU must be used. To overcome this problem, it may be advantageous to use low-contact transport mechanisms such as ultrasonic levitation [17] or walking beam transport with suitable contact material.

Assuming that the number and size of particles in the examined area are valid for the entire ring-shaped area, the particle area coverage calculated by formula (1) was extended to the entire ring defect using the measured width of the particle-containing stripe. To ensure comparability of particle area coverages, these have been related to the largest ring area, i.e., handling at 145 °C with PU as the contact material. This particle area coverage for a complete ring increases with temperature for both materials. The comparison of the two contact materials shows that the particle area coverage is always higher for the samples handled with PU. The particle area coverage of PU reaches 0.2% at RT, in contrast it stays clearly below 0.1% for PEEK at 145 °C. With the obtained particle area coverage, it is possible to make a correlation between them and the PL intensities at these handled areas. The minimum value and standard deviation of the normalized PL intensity at the contact point of the suction cups to the wafer are compared with the temperature-dependent particle area coverage in Figure 7. An exponential fit shows an exponentially decreasing correlation of normalized PL intensity with particle area coverage. Two assumptions were made. First, a normalized PL intensity of one is assumed at a particle area coverage of 0%. Second, the exponential function is fit against a limit value correspond-

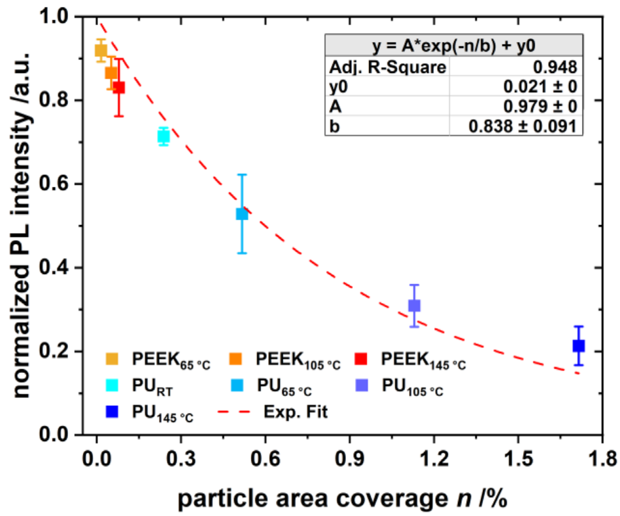

Fig. 7. Correlation of normalized PL intensity at the contact point with suction cups to the temperature and material dependent particle density.

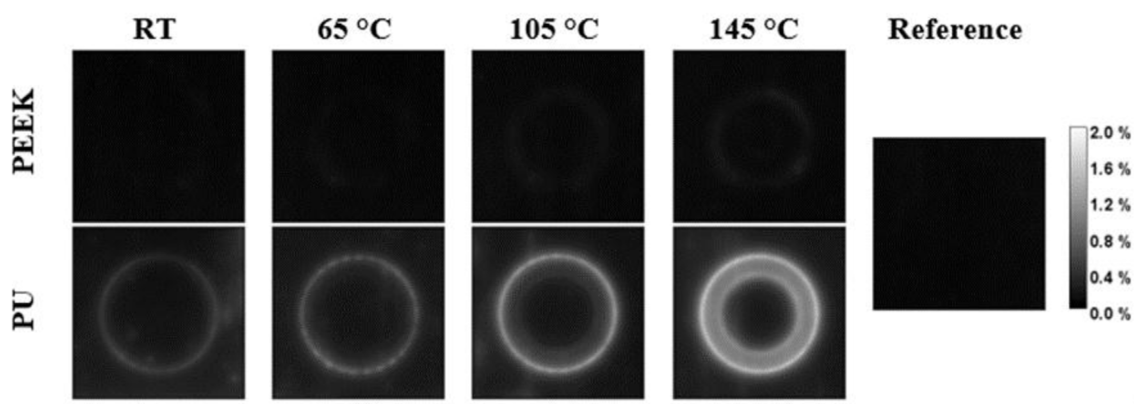

Fig. 8. Region of interest of particle area coverage calibrated PL images.

ing to the minimum value of the measurement chuck in the PL system. This fit function allows normalized PL images to be converted to particle area coverage calibrated PL images. Such a conversion can be seen in Figure 8 for the PL images of the region of interest in Figure 2.

3.2 Correlation of particle density and pseudo efficiency

In this section, the obtained particle area coverage is correlated with the relative loss in pseudo efficiency. Figure 9 shows the region of interest of characteristic defects from normalized averaged η_{Pseudo}-images. These images were generated from at least eight η_{Pseudo}-images, normalized to their maximum value. As for the PL images a ring with lower values can be seen for wafers handled with PEEK as contact material starting at a temperature of 65 °C. The same is true for wafers handled with PU as contact material, while the circular defect is already seen at RT. With increasing temperature lower η_{Pseudo} values are obtained in the ring defect and the affected area becomes larger. This is more pronounced for wafers handled with PU as the contact material.

To calculate relative η_{Pseudo} losses, the average η_{Pseudo} value in an area shown in Figure 10 is related to the location of the maximum η_{pseudo} value of each sample. The area used is about 800 mm^2 in size. The results of the local loss analysis for no handling (REF) and handling with PU or PEEK as the contact material and different temperatures are shown in Figure 11. When comparing the reference samples with the samples handled at RT with PEEK as the contact material, a loss of nearly 1%$_{\text{rel}}$ can be seen in each case. This leads to two conclusions. First, it can be said that there is an offset that deviates from the maximum value of the respective samples. In addition to the transfer of particles by handling with suction cups, other local defects

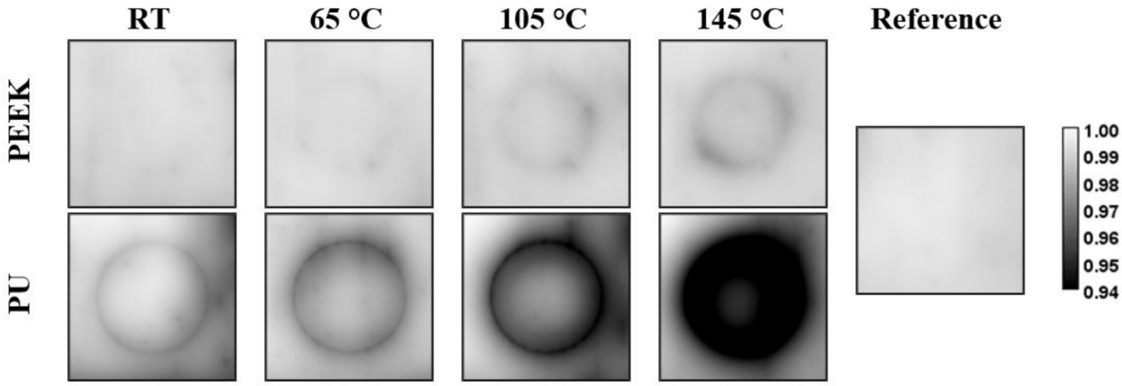

Fig. 9. Region of interest of normalized, averaged and η_{pseudo} calibrated PL images at the area grasped.

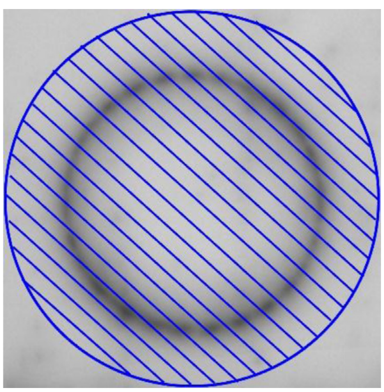

Fig. 10. Visualization of the area used to calculate the relative losses in η_{Pseudo}. The used area has a size of about 800 mm^2.

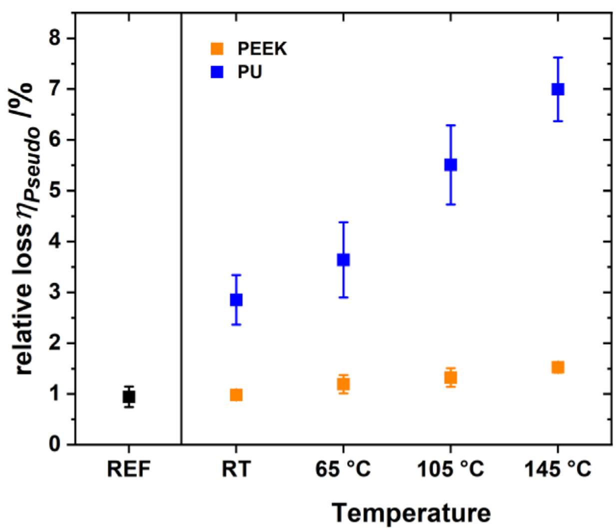

Fig. 11. Loss in η_{Pseudo} inside the used area relative to the maximum η_{Pseudo} value of the respective sample.

can be induced during the manufacturing process, which lead to a reduction in the electrical quality. Second, it can be said that handling at RT with PEEK as contact material does not cause significant particle carryover that would affect η_{pseudo}. With increasing temperature, a reduction of the pseudo-efficiency can be seen. Higher losses are induced by the handling with PU as the contact material, starting at RT. For both PEEK and PU as contact material a linear trend of relative losses in η_{pseudo} can be seen with increasing temperature. Starting at 65 °C, the relative loss for wafers handled with PEEK as contact material is 1.2$\%_{\text{rel}}$ in the used area and increases to 1.5$\%_{\text{rel}}$ at 145 °C. With PU as the contact material the relative loss is 2.9$\%_{\text{rel}}$ at RT and increases to 7$\%_{\text{rel}}$ at 145 °C.

To relate these results to the temperature dependent particle transfer findings, particle area coverage values were obtained by measuring the average particle area coverage in Figure 8 using the area of Figure 10. These obtained values in relation to the relative η_{Pseudo} losses are shown in Figure 12. To estimate the ratio of particle area coverage to losses in η_{Pseudo}, a linear fit is plotted, assuming that a particle area coverage of zero results in no losses. This fit shows, that if the particle area coverage is increased by 0.1%, the relative η_{Pseudo} loss increases by over 1.2% in

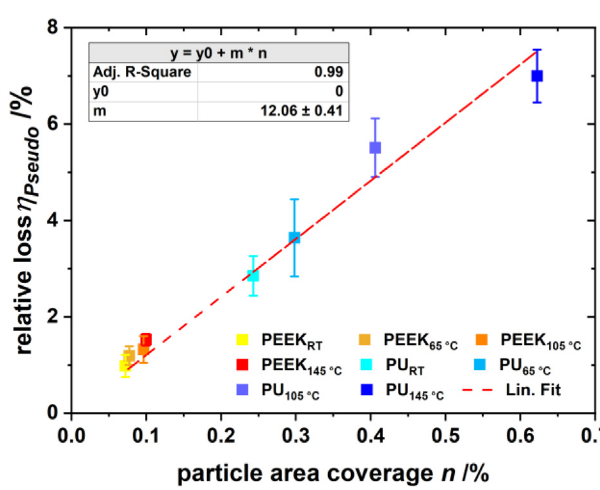

Fig. 12. Correlation of normalized η_{Pseudo} loss around a handling induced defect to the temperature and material dependent particle density.

the investigated range. Extrapolating these results to the case of four suction cups handling a M6 wafer at 145 °C, suction cups with PEEK contact material would reduce a potential efficiency of 24% by 0.05%, while suction cups with PU contact material would reduce it by 0.2%. It should be noted that this result is a conservative estimate due to the overestimation of pFF values and therefore pseudo efficiencies in the SunsPL method. Nevertheless, this relationship can be used to estimate and classify local intensity losses in PL images with respect to their effect at the cell level. The procedure can be as follows: normalize a PL image to its maximum intensity value, convert this image to a particle density calibrated PL image with the fit of Figure 7, measure the average particle area coverage in an area of about 800 mm^2 around a defect, and obtain the corresponding relative η_{Pseudo} loss from the fit of Figure 12.

4 Conclusion

In this work, a correlation of particle area coverage resulting from material carryover from used vacuum cups with normalized PL intensities and normalized pseudo efficiencies has been demonstrated. PL imaging, SEM and SunsPL imaging were used to obtain these results. Two vacuum cups contact materials with different properties, PEEK and PU, were used to find particle area coverages ranging from 0.01% to 1.71% in characteristic imprints, seen as lower intensities in PL images. This was achieved not only by using different materials, but also by varying the temperature. It was discussed that the main property of particle transfer for materials in contact with the sensitive silicon surface is the temperature dependent hardness. As the temperature increases, more particles are transferred because of plastic deformation for thermoplastics and higher abradability for elastomers. With the particle area coverage an exponential correlation to normalized PL intensities at the contact point with suction cups was shown. Using the SunsPL imaging technique, relative pseudo efficiency losses were calculated around a characteristic imprint with lower values for an area of about 800 mm^2. Using these loss values and the calculated particle area coverages in this area, a correlation between the particle area coverage and the pseudo efficiency loss has been pointed out. A linear trend was used to conservatively fit this correlation. As the particle area coverage increases by 0.1%, the relative η_{Pseudo} decreases by over 1.2%. These results can be used to predict the efficiency loss due to organic particle transfer for specific contact points using only a standard photoluminescence image. This research applies not only to suction cups, but to all wafer contacts with potential organic particle transfer prior to a-Si deposition. This includes automation and chemical carriers, conveyor belts, wafer flippers, walking beams, or tray carriers.

Part of this work was funded by German Federal Ministry for Economic Affairs and Energy under contract number 03EE1096A (Salsa) and 03EE1001A (NextTec).

Author contribution statement

All authors contributed equally to the paper.

References

1. K. Reddig, Photovolt. Int. **4**, 18 (2009)
2. J.J. Haase, in: *Proceedings of the IEEE 4th World Conference on Photovoltaic Energy Conversion* (Waikoloa, 2006), p. 1256
3. M. Schilp, Ph.D. thesis, TU Munich, 2006
4. A. Grubba, Ph.D. thesis, University of Dortmund, 2002
5. VDMA, *International Technology Roadmap for Photovoltaic (ITRPV)*, 13th Edition, (VDMA, 2022)
6. H. Angermann, Appl. Surf. Sci. **312**, 3 (2014)
7. A. Fischer et al., AIP Conf. Proc. **2147**, 050002 (2019)
8. A. Fischer et al., in *Proceedings of the 36th Eur. Photovolt. Sol. Energy Conf. Exhib.* (Marseille, 2019), p. 541
9. V. Giglia et al., Prog. Photovolt. Res. Appl. **28**, 1333 (2020)
10. A. Fischer et. al., EPJ Photovolt. **13**, 14 (2022)
11. B. Michl et al., Prog. Photovolt. : Res. Appl. **22**, 581 (2014)
12. N. Iyer et. al., IEEE Trans. Semicond. Manufact. **14**, 85 (2001)
13. T.C. Ovaert et al., Wear **150**, 275 (1991)
14. J.F. Archard, J. Appl. Phys. **24**, 981 (1953)
15. L. Chang et al., Tribol. Lett. **65**, 1 (2017)
16. V.L. Popov, in *Kontaktmechanik und reibung* (Springer, Berlin, Heidelberg, 2010)
17. G. Reinhart et al., in: *2011 IEEE/SEMI Advanced Semiconductor Manufacturing Conference* (2011), pp. 1–6

Cite this article as: Andreas Fischer, Ioan Voicu Vulcanean, Sebastian Pingel, Anamaria Steinmetz, Impact of organic particles from wafer handling equipment on silicon heterojunction pseudo-efficiency, EPJ Photovoltaics 14, 29 (2023)